# Matlab/Simulink 1D model of longitudinal wave propagation through piezoceramic rings

Igor Jovanović and Dragan Mančić

*Abstract*— **One-dimensional (1D) model of piezoelectric elements enable fast prediction of performance, as well as a good insight into the behaviour of piezoelectric elements and the entire ultrasonic transducer during operation. In this paper, the Matlab/Simulink 1D model of piezoceramic rings that include only thickness oscillation modes is presented, while radial oscillations are neglected. Implementation of equivalent electromechanical circuits in the modelling of piezoelectric elements did not bring a larger amount of information in relation to the number of information obtained by applying constitutive piezoelectric equations. In addition, the presented model that directly relies on the constitutive piezoelectric equations enables better visualization of wave propagation through transducer structure. The input electrical impedances for piezoceramic rings are calculated using the realized model and then compared with experimental results to validate the model.**

*Index Terms*— **Piezoceramic ring, Matlab/Simulink model, Input electrical impedance.**

## I. Introduction

Models involving computer simulations have become an essential part of the transducer design process. Electromechanical equivalent circuits are frequently used to model and analyse ultrasonic transducers, whose application is based on the idea that wave propagation speed is equivalent to electric current, while mechanical force is equivalent to electric voltage [1]. Today, many transducers are designed with one dominant resonant mode, which can further simplify the models and justify their use. Piezoceramic rings of different thicknesses and inner/outer diameters are widely used as active components in ultrasonic sandwich piezoceramic transducers [2].

In case that the axial dimensions of ultrasonic transducers that oscillate in the thickness mode are larger than the radial dimensions, one-dimensional analysis can be applied in the modelling process of both piezoceramic rings and whole sandwich transducers [3], [4]. Although this dimensional relationship is common with most ultrasonic transducers, in the process of modelling transducers with a complex structure (e.g. composite transducers), it is important to predict the behaviour of transducers in all directions of oscillation propagation [5]. In this case, it is necessary to use three-dimensional models [6]. The components of these power transducers can be modelled by mathematical analysis with the help of appropriate physical laws.

In this paper, the Matlab/Simulink model of piezoceramic rings based on constitutive equations of piezoelectric effect is presented. The proposed Matlab/Simulink model leads to simpler implementation than the mathematical model. This model can also be used to analyse multilayer structures that include both piezoelectric materials and metal endings.

## II. Description of Governing Equations

Constitutive equations for piezoelectric material can be written in the following form when neglecting transverse dimensions [7]:

$$E = -hS + \frac{D}{\varepsilon^S}, \tag{1}$$

$$T = c^D S - hD, \tag{2}$$

where the mechanical stress $T$ can be determined by dividing the total extension or compression force $F$ by the transverse surface $P$, $T=F/P$. $E$ is the applied electrical field, $S$ is the mechanical deformation, $D$ is the dielectric displacement, $c^D$ is the elastic stiffness coefficient, $h$ and $\varepsilon^S$ describe physical characteristics of piezoelectric material.

By applying Newton's II law, which defines force as a product of mass and acceleration, and using mass as a product of volume and density, mechanical stress is expressed as:

$$T = \rho l \frac{\partial^2 u}{\partial t^2}, \tag{3}$$

where $\rho$ is the density, $l$ is the thickness of the piezoelectric material, and $u$ are the mechanical displacements components. By differentiating the last equation along the $z$-axis, it is obtained [8]:

$$\frac{\partial T}{\partial z} = \rho \frac{\partial^2 u}{\partial t^2}. \tag{4}$$

Expressing Hook's law in the following form [9]:

$$T = c^D \frac{\partial u}{\partial z}, \tag{5}$$

where the elastic stiffness coefficient $c^D$ represents the coefficient of proportionality. The previous expression can be

Igor Jovanović and Dragan Mančić are with the University of Niš, Faculty of Electronic Engineering, 14 Aleksandra Medvedeva, 18000 Niš, Serbia (e-mail: igor.jovanovic@elfak.ni.ac.rs and dragan.mancic@elfak.ni.ac.rs).

rewritten using the propagation speed of longitudinal waves in a thin cylinder $v^2=c/\rho$, as:

$$\frac{\partial^2 u}{\partial t^2} = v^2 \frac{\partial^2 u}{\partial z^2}. \tag{6}$$

In 1D models, only mechanical deformation and divergence of the dielectric displacement along the $z$-axis are of interest:

$$S = \frac{\partial u}{\partial z}, \text{ and } \nabla D = \frac{\partial u}{\partial z} = 0. \tag{7}$$

By differentiating expression (2) along the $z$-axis, one may obtain:

$$\frac{\partial T}{\partial z} = c^D \frac{\partial^2 u}{\partial z^2} - h\frac{\partial D}{\partial z}. \tag{8}$$

By solving (6) in the general case, the equation of nonstationary wave motion is obtained in the form of a linear differential equation of the second-order with two independent variables (by $z$-axis and by time $t$).

If a multilayer structure shown in Fig. 1(a) is observed, the solution of this hyperbolic partial differential equation (determinant is $4v^2 > 0$) can be written in general form for layer $n$ in the multilayer structure:

$$u_n = \alpha_n e^{-j\omega \Delta t_n} + \beta_n e^{j\omega \Delta t_n}. \tag{9}$$

Amplitudes of the mechanical displacements components in the direction of wave propagation are denoted by $\alpha_n$, and in the opposite direction to the direction of wave propagation by $\beta_n$, on the surface of the $n$-th layer. The ultrasonic wave propagation time through the $n$-th piezoelectric layer is equal to the ratio of the length of the propagation path and the speed of wave propagation (for propagation through the entire layer $\Delta t_n = l_n/v_n$).

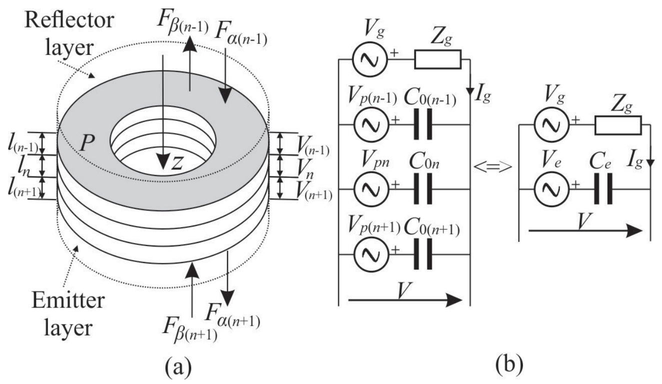


Fig. 1. (a) Multilayer structure of an ultrasonic sandwich piezoceramic transducer, (b) its equivalent circuit in the case of a parallel electrical excitation.

To obtain the analytical expression for the electric voltage $V_n$ on the $n$-th piezoelectric layer, (1) can be written in the following form:

$$E_n = -h_n \frac{\partial u_n}{\partial z} + \frac{Q_n}{P\varepsilon_n^S}, \tag{10}$$

for $D=Q_n/P$ and static capacitance of the $n$-th layer $C_{0n}=\varepsilon_n^S P/l_n$. $Q_n$ is the amount of accumulated charge stored on capacitor $C_{0n}$.

By integrating the last equation along the $z$-axis the following expression was obtained [9]:

$$\begin{aligned} V_n &= -h_n \int_0^{l_n} \frac{\partial u_n}{\partial z} dz + \frac{Q_n}{P\varepsilon_n^S} \int_0^{l_n} dz = \\ &= -h_n \left[ \alpha_n \left( e^{-j\omega\Delta t_n} - 1 \right) + \beta_n \left( e^{-j\omega\Delta t_n} - 1 \right) \right] + \frac{Q_n}{C_{0n}}. \end{aligned} \tag{11}$$

Is useful to introduce mechanical displacements components $u_n$ with the help of forces acting on the surfaces, which are perpendicular to the $z$-axis ($F_{\alpha n}$ and $F_{\beta n}$) [9]:

$$V_n = -\frac{h_n}{j\omega Z_{cn}} \left( F_{\alpha_n} + F_{\beta_n} \right) \left( 1 - e^{-j\omega\Delta t_n} \right) + \frac{Q_n}{C_{0n}}, \tag{12}$$

where the specific acoustic impedance $Z_{cn}$ and the amplitudes of the mechanical displacements components are represented as:

$$Z_{cn} = \frac{c_n^D P}{v_n}, \ \alpha_n = -\frac{F_{\alpha_n}}{j\omega Z_{cn}} \text{ and } \beta_n = \frac{F_{\beta_n}}{j\omega Z_{cn}} e^{-j\omega\Delta t_n}. \tag{13}$$

The general analysis of the multilayer structure of an ultrasonic sandwich piezoceramic transducer includes several piezoelectric layers that act as sources or as sensors of oscillations. However, in this paper, the analysis is limited to the most commonly used electrical connection of piezoelectric layers in practice, to the analysis of single-layer or multilayer structures that are mechanically connected in series and electrically excited in parallel, Fig. 1(a). Fig. 1(b) shows that the voltage $V$ of the parallel connection of all active layers consists of voltage contributions based on the piezoelectric effect $V_{pn}$ and the amount of accumulated charge stored on capacitor $C_{0n}$. The equivalent capacitance of the parallel connection of $N$ piezoelectric layers $C_e$, as well as the total amount of charge $Q_e$, which depends on the voltage of the electric generator $V_g$, and its impedance $Z_g$, can be represented by the expressions:

$$C_e = \sum_{n=1}^{N} C_{0n}, \ Q_e = \frac{V_g - V}{j\omega Z_g}. \tag{14}$$

When the equivalent circuit of Fig. 1(b) is considered as a capacitive voltage divider, the equivalent voltage generated by the piezoelectric effect can be calculated as follows [10]:

$$V_e = \frac{V_g}{1 + j\omega Z_g C_e} - \\ - \frac{j\omega Z_g C_e}{1 + j\omega Z_g C_e} \sum_{n=1}^{N} \frac{C_{0n}}{C_e} \frac{h_n}{j\omega Z_{cn}} \left( F_{\alpha_n} + F_{\beta_n} \right) \left( 1 - e^{-j\omega \Delta t_n} \right). \tag{15}$$

If the structure has only one active layer, then the voltage on it is calculated by the expression:

$$V = \frac{1}{1 + j\omega Z_g C_0} \left[ V_g - j\omega Z_g C_0 \frac{h_n}{j\omega Z_c} \left( F_\alpha + F_\beta \right) \left( 1 - e^{-j\omega \Delta t} \right) \right]. \tag{16}$$

It is necessary to present mechanical deformation $S$ in (2) as a derivative of mechanical displacements components $u$ along the $z$-axis (7), and use expressions (13) for amplitudes of the mechanical displacements components to obtain analytical expressions for forces acting on piezoceramic surfaces [11]:

$$F_n = c_n^D P \frac{j\omega}{v_n} \left( \frac{F_{\alpha_n}}{j\omega Z_{cn}} e^{-j\omega \Delta t_n} + \frac{F_{\beta_n}}{j\omega Z_{cn}} \right) - h_n Q_n. \tag{17}$$

Equation (17) is an expression for the force on the external surfaces (perpendicular to the $z$-axis) of the $n$-th layer in the observed piezoceramic structure, in general form. Boundary conditions can be expressed based on continuity of forces and mechanical displacements components on contact surfaces:

$$F_n \big|_{z=l_n} = F_{n+1} \big|_{z=0} \text{ and } u_n \big|_{z=l_n} = u_{n+1} \big|_{z=0}. \tag{18}$$

When the ultrasonic wave passes from one layer to another, the speed of propagation changes. For explicit analysis of forces acting on the boundary surfaces between two layers, it is necessary to define the transmission and reflection coefficients during the passage of an ultrasonic wave from one layer ($n$) to another ($n$+1) [12]:

$$T_n^{n+1} = \frac{2 Z_{c(n+1)}}{Z_{c(n+1)} + Z_{cn}} \text{ and } R_n^{n+1} = \frac{Z_{c(n+1)} - Z_{cn}}{Z_{c(n+1)} + Z_{cn}}. \tag{19}$$

Components of mechanical forces acting on boundary surfaces, with defined boundary conditions and taking into account the transmission and reflection of the ultrasonic waves, can be presented by the following expressions:

$$F_{\alpha_n} = \frac{1}{1 - T_{n-1}^n K_n} \Big[ F_{\alpha_{(n-1)}} T_{n-1}^n \left( e^{-j\omega \Delta t_{(n-1)}} - K_{n-1} \right) - F_{\beta_{(n-1)}} T_{n-1}^n K_{n-1} + \\ + F_{\beta_n} \left( R_n^{n-1} e^{-j\omega \Delta t_n} + T_{n-1}^n K_n \right) + \\ + \frac{T_{n-1}^n V}{2} \left( h_n C_{0n} - h_{n-1} C_{0(n-1)} \right) \Big], \tag{20}$$

$$F_{\beta_n} = \frac{1}{1 - T_{n+1}^n K_n} \Big[ F_{\beta_{(n+1)}} T_{n+1}^n \left( e^{-j\omega \Delta t_{(n+1)}} - K_{n+1} \right) - F_{\alpha_{(n+1)}} T_{n+1}^n K_{n+1} + \\ + F_{\alpha_n} \left( R_n^{n+1} e^{-j\omega \Delta t_n} + T_{n+1}^n K_n \right) + \\ + \frac{T_{n+1}^n V}{2} \left( h_n C_{0n} - h_{n+1} C_{0(n+1)} \right) \Big], \tag{21}$$

wherein $K_n = h_n^2 C_{0n} \frac{1 - e^{-j\omega \Delta t_n}}{2 j\omega Z_{cn}}$.

Indices in (20) and (21) indicate that for the first layer ($n = 1$) and the last layer ($n = N$), the values with indices $n - 1 = 0$ and $n + 1 = N + 1$, refer to the propagation medium behind the reflector layer and in front of the emitter layer, respectively.

The components of mechanical forces on the surfaces of the unloaded piezoceramic transducer that consists of only one piezoceramic layer (the influence of external forces on the transducer is equal to zero $F_{\alpha 0}=F_{\beta 2}=0$) are calculated as:

$$F_{\alpha_1} = \frac{1}{1 - T_0^1 K} \left[ F_{\beta_1} \left( R_1^0 e^{-j\omega \Delta t_1} + T_0^1 K \right) + \frac{T_0^1 V}{2} h C_0 \right], \tag{22}$$

$$F_{\beta_1} = \frac{1}{1 - T_2^1 K} \left[ F_{\alpha_1} \left( R_1^2 e^{-j\omega \Delta t_1} + T_2^1 K \right) + \frac{T_2^1 V}{2} h C_0 \right]. \tag{23}$$

Since this paper shows the modelling of only one active layer, which is unloaded (surrounding medium is air), external acoustic impedances are 400 Rayl, [11]. The value used for external acoustic impedances is much less than the specific acoustic impedance of the active layer, so it can be considered $T_n^{n+1} = 2$ and $R_n^{n+1} = -1$.

## III. Simulation and Experimental Results

Expressions (15), (20) and (21) can form a system of equations that describes the electromechanical structure shown in Fig. 1. By solving this system of equations, numerical results are obtained that represent the mechanical forces in each of the layers of the packet transducer. In addition to knowing the characteristics of the electric generator, it is possible to calculate the input electrical impedance of the transducer itself.

Fig. 2 shows the Matlab/Simulink 1D model of one piezoceramic layer (a model of longitudinal wave propagation through piezoceramic rings). The model represents a system of equations formed by the Laplace transform (with related expressions for impulse delays $e^{-\tau s}$, differentiations $s$, and integrations $1/s$ with respect to time) of terms (16), (22) and (23).

The calculated and experimental results are obtained using a piezoceramic equivalent material. The dimensions of the used piezoceramic rings are given in the Table I, where $l$ is the thickness, $b$ and $a$ are the inner and outer diameters of lead zirconate titanate (PZT) piezoceramic rings.

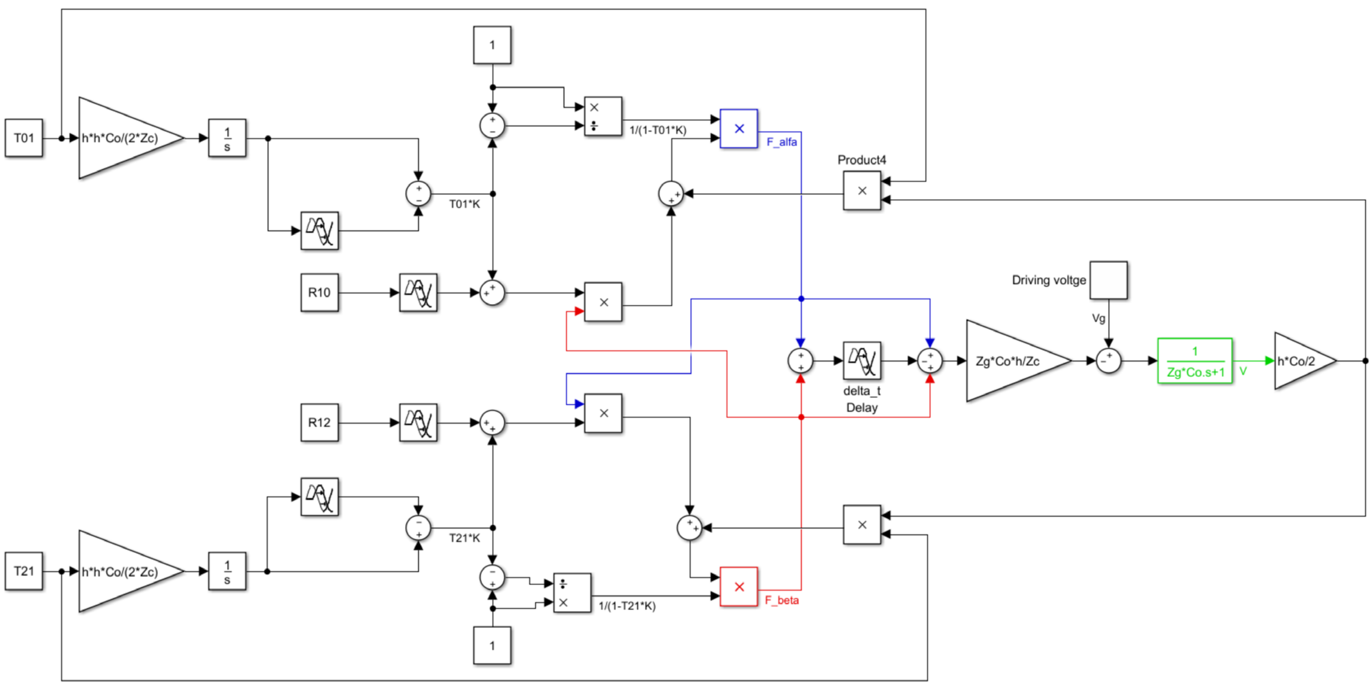

Fig. 2. Matlab/Simulink model of the piezoceramic ring.

Three samples of commercial PZT4 rings and three samples of commercial PZT8 rings have been characterized [13]. The electrical impedance measurements are conducted using an HP 4194A Network Impedance Analyzer.

TABLE I
PIEZOCERAMIC RING DIMENSIONS

| Sample | *a* (mm) | *b* (mm) | *l* (mm) | *PZT equivalent material* [11] |
|---|---|---|---|---|
| I | 38 | 15 | 5 | PZT4 |
| II | 38 | 13 | 6.35 | PZT4 |
| III | 50 | 20 | 6.35 | PZT4 |
| IV | 24 | 15 | 3 | PZT8 |
| V | 38 | 13 | 6 | PZT8 |
| VI | 10 | 4 | 2 | PZT8 |

As shown in Figs. 3-8, the measured frequency characteristic corresponds with the simulated curves using the proposed model. The proposed 1D model predicts only thickness modes while does not consider other mods. The images show the first thickness resonant mode for all used PZT samples.

The model acts as a three-port network whose ports refer to mechanical forces ($F_{alfa}$ and $F_{beta}$) acting on the circular-ring surfaces of the piezoceramic ring, and the third port represents the electrical driving voltage ($V_g$). The charge components are proportional to the difference of mechanical displacements components between circular-ring surfaces and can be obtained including the equation (14) in the model.

These charge components further cause secondary forces to propagate through the transducer and the surrounding medium. The secondary piezoelectric effect was modelled using two positive feedback loops in Fig. 2.

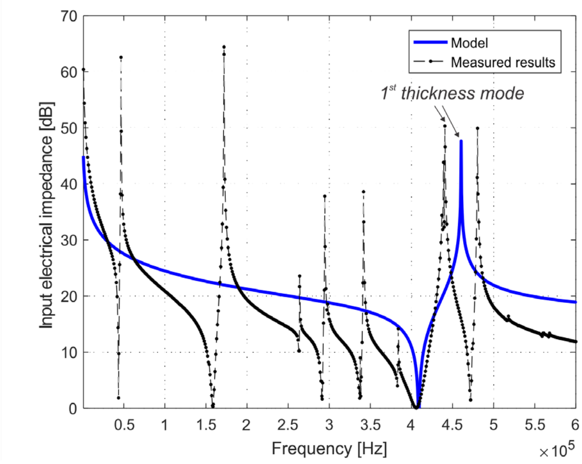

Fig. 3. Simulated and experimental input electrical impedance versus frequency for the I sample.

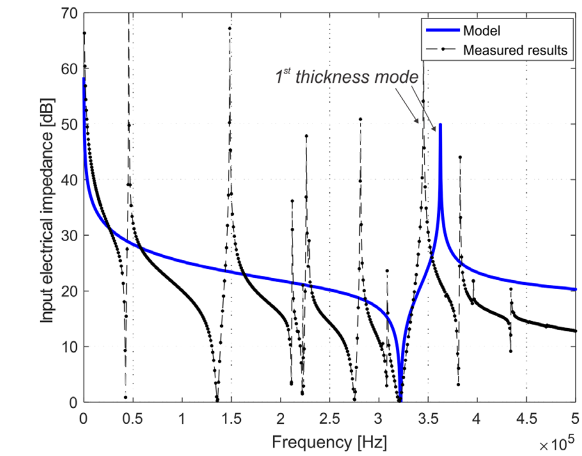

Fig. 4. Simulated and experimental input electrical impedance versus frequency for the II sample.

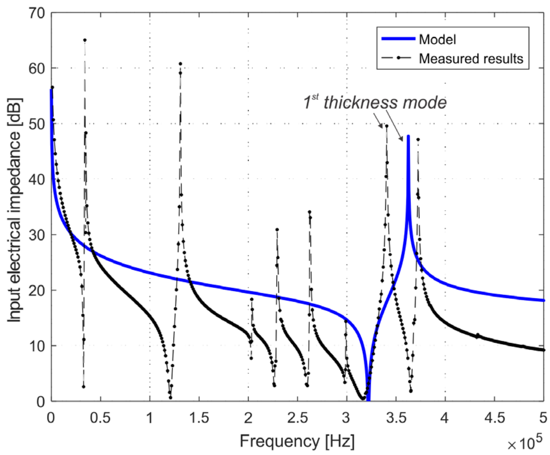


Fig. 5. Simulated and experimental input electrical impedance versus frequency for the III sample.

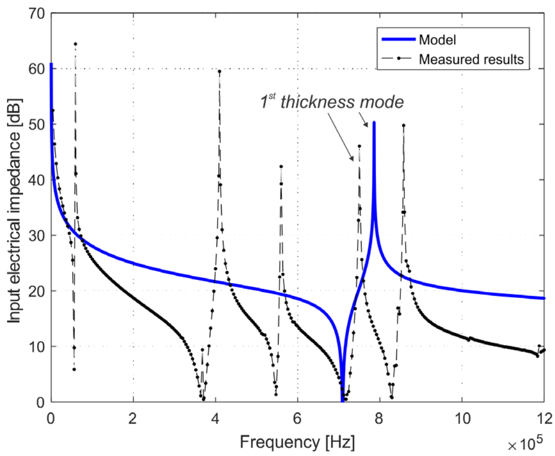


Fig. 6. Simulated and experimental input electrical impedance versus frequency for the IV sample.

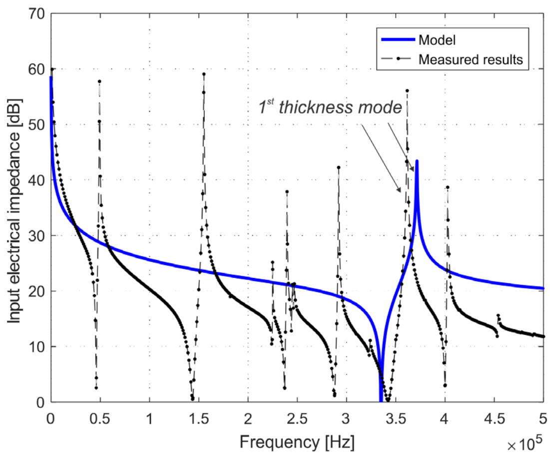


Fig. 7. Simulated and experimental input electrical impedance versus frequency for the V sample.

The driving current $I_g$ from Fig. 1(a) was obtained by differentiating the charge components $I_g=sQ$. The input electrical impedance was obtained by dividing the voltage $V$ from expression (16) and driving current.

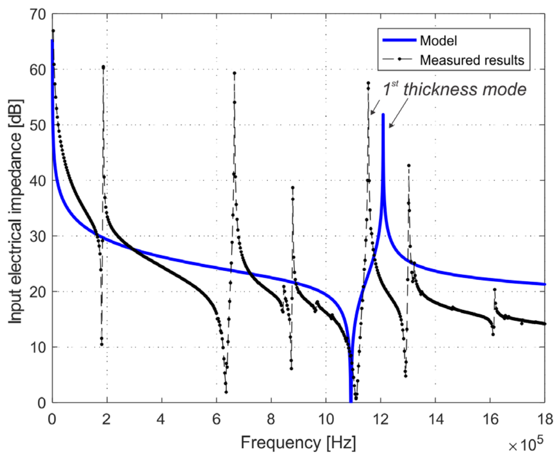


Fig. 8. Simulated and experimental input electrical impedance versus frequency for the VI sample.

## IV. Conclusion

The piezoceramic rings with different dimensions are analysed using the developed model. Verification of the proposed model is performed by comparing the modelled dependencies of input electrical impedance vs. frequency with the experimental results. The matching of experimental and theoretical results is quite good and validates the proposed model. The presented model predicts thickness oscillatory modes of PZT piezoceramic rings taking the interaction with the surrounding media into account. The model describes the behaviour of the piezoceramic ring with two mechanical ports (one for each external surface normal to the z-axis) and one electrical port.

This approach is suitable for the analysis of the completely multilayer structure of the transducer. When calculating the forces acting on the passive layers of the transducer (materials that do not have piezoelectric properties), it is necessary to adopt that $h$=0.

This approach is not only effective in terms of computation time but also in reducing difficulties associated with the calibration of material parameters. Errors in predicting thickness oscillatory modes can be reduced by fitting the parameters of the piezoceramic material.

## Acknowledgment

This work has been supported by the Ministry of Education, Science and Technological Development of the Republic of Serbia.

## References

[1] D. Mančić, M. Radmanović, “Piezoceramic ring loaded on each face: a three-dimensional approach," Electronic Journal "Technical acoustics", vol. 2, pp. 1.1-1.7, 2002.

[2] I. Jovanović, D. Mančić, V. Paunović, M. Radmanović, Z. Petrušić, “A Matlab/Simulink Model of Piezoceramic Ring for Transducer Design," ICEST, Niš, Serbia, vol. 3, pp. 952-955, 2011.

[3] W. P. Mason, *Electromechanical Transducers and Wave Filters*, Princeton: Van Nostrand, 1948.

[4] A. Abdullah, M. Shahini, A. Pak, “An approach to design a high power piezoelectric ultrasonic transducer," J. Electroceram. vol. 22, pp. 369–382, 2009.
[5] I. Jovanović, D. Mančić, U. Jovanović, M. Prokić, “A 3D model of new composite ultrasonic transducer, "Journal of Computational Electronics, vol. 16, no. 3, pp. 977-986, 2017.
[6] D. Mančić, G. Stančić, “New Three-dimensional Matrix Models of the Ultrasonic Sandwich Transducers, "Journal of Sandwich Structures & Materials, vol. 12, pp. 63-80, 2010.
[7] Z. H. Zhang, B. Y. Sun, L. P. Shi, “Theoretical and Experimental Study on Secondary Piezoelectric Effect Based on PZT-5,” Phys.: Conf. Ser. vol. 48, pp. 86-90, 2016
[8] U. Jovanović, Lj. Perić, I. Jovanović, D. Mančić, “Analisys of longitudinal oscillations of Free prismatic piezoceramic beams", 24th International Conference "Noise and Vibration", Niš, Serbia, pp. 229 - 235, 29-31. October 2014.
[9] S. Cochran, C. E. M. Demore, C. R. P. Courtney, “Modelling ultrasonic transducer performance: one dimensional models," in *Ultrasonic transducers: materials and design for sensors, actuators and medical applications*, Cambridge: Woodhead Publishing Ltd, 2012. pp. 187-219.
[10] J. L. Dion, E. Cornieles, F. Galindo, K. Agbossou, “Exact one-dimensional computation of ultrasonic transducers with several piezoelectric elements and passive layers using the transmission line analogy, "IEEE Transactions on Ultrasonics Ferroelectrics and Frequency Control, vol. 44, no. 5, pp. 112031, 1997.
[11] I. Jovanović, “New Power Composite Ultrasonic Transducers,” Ph.D. dissertation (in Serbian), University of Niš, Faculty of Electronic Engineering, Niš, Serbia, 2018
[12] G. Hayward, M. N. Jackson, “A lattice model of the thickness-mode piezoelectric transducer," IEEE Trans. Ultrason. Ferroelec. Freq. Contr. Vol. 33, No. 1, pp. 41-50, 1986.
[13] *Technical Publication TP-226*, Morgan Electro Ceramics.